

POLITECNICO DI TORINO
Repository ISTITUZIONALE

1306-km 20x1248-Gb/s PM-64QAM Transmission over PSCF with Net SEDP 11,300 (bkm)/s/Hz using 115 samp/symb DAC

Original

1306-km 20x1248-Gb/s PM-64QAM Transmission over PSCF with Net SEDP 11,300 (bkm)/s/Hz using 115 samp/symb DAC / A., Nespola; S., Straullu; Bosco, Gabriella; Carena, Andrea; Jiang, Yanchao; Poggiolini, Pierluigi; F., Forghieri; Y., Yamamoto; M., Hirano; T., Sasaki; J., Bauwelinck; K., Verheyen. - In: OPTICS EXPRESS. - ISSN 1094-4087. - ELETTRONICO. - 22:1(2014), pp. 1796-1805. [10.1364/OE.22.001796]

Availability:

This version is available at: 11583/2542089 since:

Publisher:

OSA Optical Society of America

Published

DOI:10.1364/OE.22.001796

Terms of use:

This article is made available under terms and conditions as specified in the corresponding bibliographic description in the repository

Publisher copyright

(Article begins on next page)

1306-km 20x124.8-Gb/s PM-64QAM Transmission over PSCF with Net SEDP 11,300 (b·km)/s/Hz using 1.15 samp/symb DAC

A. Nespola,^{1,*} S. Straullu,¹ G. Bosco,² A. Carena,² J. Yanchao,² P. Poggiolini,²
F. Forghieri,³ Y. Yamamoto,⁴ M. Hirano,⁴ T. Sasaki,⁴ J. Bauwelinck⁵ and K. Verheyen⁵

¹Istituto Superiore Mario Boella, via Pier Carlo Boggio 61, 10138 Torino, Italy

²Politecnico di Torino, DET, corso Duca degli Abruzzi, 24, 10129 Torino, Italy

³Cisco Photonics Italy srl, via Philips 12, 20900 Monza, Italy

⁴Sumitomo Electric Industries, LTD, 1, Taya-cho, Sakae-ku, Yokohama, 244-8588, Japan

⁵INTEC/IMEC, Ghent University, Sint-Pietersnieuwstraat 41, 9000 Ghent, Belgium

*nespola@ismb.it

Abstract: We demonstrated the transmission of a Nyquist-WDM signal based on PM-64QAM modulation in an EDFA-only submarine configuration composed of 54.4 km-long fiber spans: 20 channels at 124.8-Gb/s were propagated over 1306 km of low-loss pure-silica-core fiber (PSCF). Thanks to an aggressive digital spectral shaping, we achieved a raw spectral efficiency (SE) of 10.4 b/s/Hz, corresponding to 8.67 b/s/Hz net SE when considering a 20% FEC overhead. Transmitter DACs are operated at a record-low 1.15 samples/symbol, enabled by the insertion of advanced anti-alias filters. The achieved SE-times-distance product was 11,327 (b·km)/(s·Hz), the highest reported so far for PM-64QAM. Combining the experimental results with the performance predictions obtained using an analytical model of nonlinear propagation in uncompensated coherent optical systems (the so-called “GN-model”), we show that PM-64QAM is a realistic option for ultra-high capacity systems in the 1,000 km range, carrying up 40 Tb/s in the C-band.

©2014 Optical Society of America

OCIS codes: (060.0060) Fiber optics and optical communications; (060.1660) Coherent communications; (060.4080) Modulation; (060.2360) Fiber optics links and subsystems.

References and links

1. J. Renaudier, G. Charlet, O. Bertran Pardo, H. Mardoyan, P. Tran, M. Salsi, and S. Bigo, “Experimental analysis of 100Gb/s coherent PDM-QPSK long-haul transmission under constraints of typical terrestrial networks,” in *Proceedings of ECOC 2008*, paper Th.2.A.3.
2. M. Salsi, H. Mardoyan, P. Tran, C. Koebele, G. Charlet, and S. Bigo, “155x100 Gbit/s coherent PDM-QPSK transmission over 7,200 km,” in *Proceedings of ECOC 2009*, paper PD2.5.
3. J.-X. Cai, Y. Cai, C. R. Davidson, D. G. Foursa, A. Lucero, O. Sinkin, W. Patterson, A. Pilipetskii, G. Mohs, and N. S. Bergano, “Transmission of 96x100G pre-filtered PDM-RZ-QPSK channels with 300% spectral efficiency over 10,608km and 400% spectral efficiency over 4,368km,” in *Proceedings of OFC 2010*, paper PDPB10.
4. E. Torrenco, R. Cigliutti, G. Bosco, G. Gavioli, A. Alaimo, A. Carena, V. Curri, F. Forghieri, S. Piciaccia, M. Belmonte, A. Brinciotti, A. La Porta, S. Abrate, and P. Poggiolini, “Transoceanic PM-QPSK terabit superchannel transmission experiments at Baud-Rate subcarrier spacing,” in *Proceedings of ECOC 2010*, paper We.7.C.2.
5. J.-X. Cai, Y. Cai, Y. Sun, C. R. Davidson, D. G. Foursa, A. Lucero, O. Sinkin, W. Patterson, A. Pilipetskii, G. Mohs, and N. S. Bergano, “112x112 Gb/s transmission over 9,360 km with channel spacing set to the Baud rate (360% spectral efficiency),” in *Proceedings of ECOC 2010*, paper PD2.1.
6. D. Foursa, Y. Cai, J.-X. Cai, C. Davidson, O. V. Sinkin, W. T. Anderson, A. Lucero, A. Pilipetskii, G. Mohs, and N. S. Bergano, “Coherent 40 Gb/s transmission with high spectral efficiency over transpacific distance,” in *Proceedings of OFC 2011*, paper OMI4.
7. X. Zhou, J. Yu, M.-F. Huang, Y. Shao, T. Wang, P. Magill, M. Cvijetic, L. Nelson, M. Birk, G. Zhang, S. Ten, H. B. Matthew, and S. K. Mishra, “32Tb/s (320 114Gb/s) PDM-RZ-8QAM transmission over 580 km of SMF-28 ultra-low-loss fiber,” in *Proceedings of OFC 2009*, paper PDPB4.
8. R. Cigliutti, E. Torrenco, G. Bosco, N. P. Caponio, A. Carena, V. Curri, P. Poggiolini, Y. Yamamoto, T. Sasaki, and F. Forghieri, “Transmission of 9x138 Gb/s prefiltered PM-8QAM signals over 4000 km of pure silica-core fiber,” *J. Lightwave Technol.* **29**(15), 2310–2318 (2011).

9. P. J. Winzer and A. H. Gnauck, "112-Gb/s polarization-multiplexed 16-QAM on a 25-GHz WDM grid," in *Proceedings of ECOC 2008*, paper Th.3.E.5.
10. A. H. Gnauck, P. J. Winzer, C. R. Doerr, and L. L. Buhl, "10 × 112-Gb/s PDM 16-QAM transmission over 630 km of fiber with 6.2-b/s/Hz spectral efficiency," in *Proceedings of OFC 2009*, paper PDPB8.
11. S. Yamanaka, T. Kobayashi, A. Sano, H. Masuda, E. Yoshida, Y. Miyamoto, T. Nakagawa, M. Nagatani, and H. Nosaka, "11 × 171 Gb/s PDM 16-QAM transmission over 1440 km with a spectral efficiency of 6.4 b/s/Hz using high-speed DAC," in *Proceedings of ECOC 2010*, paper We.8.C.1.
12. M.-F. Huang, Y.-K. Huang, E. Ip, Y. Shao, and T. Wang, "WDM transmission of 152-Gb/s polarization multiplexed RZ-16QAM signals with 25-GHz channel spacing over 15×80-km of SSMF," in *Proceedings of OFC 2011*, paper OThX2.
13. J.-X. Cai, H. G. Batshon, H. Zhang, C. R. Davidson, Y. Sun, M. Mazurczyk, D. G. Foursa, A. Pilipetskii, G. Mohs, and N. S. Bergano, "25 Tb/s Transmission over 5,530 km using 16QAM at 5.2 bits/s/Hz spectral efficiency," in *Proceedings of ECOC 2012*, paper Mo.1.C.1.
14. A. Nespola, S. Straullu, A. Carena, G. Bosco, R. Cigliutti, V. Curri, P. Poggiolini, M. Hirano, Y. Yamamoto, T. Sasaki, J. Bauwelinck, K. Verheyen, and F. Forghieri, "Extensive fiber comparison and GN-model validation in uncompensated links using DAC-generated nyquist-WDM PM-16QAM channels," in *Proceedings of OFC 2013*, paper OTh3G.5.
15. A. Sano, T. Kobayashi, A. Matsuura, S. Yamamoto, S. Yamanaka, E. Yoshida, Y. Miyamoto, M. Matsui, M. Mizoguchi, and T. Mizuno, "100 × 120-Gb/s PDM 64-QAM transmission over 160 km using linewidth-tolerant pilotless digital coherent detection," in *Proceedings of ECOC 2010*, paper PD2.2.
16. T. Kobayashi, A. Sano, A. Matsuura, M. Yoshida, T. Sakano, H. Kubota, Y. Miyamoto, K. Ishihara, M. Mizoguchi, and M. Nagatani, "45.2Tb/s C-band WDM transmission over 240km using 538Gb/s PDM-64QAM single carrier FDM signal with digital pilot tone," in *Proceedings of ECOC 2011*, paper Th.13.C.6.
17. J. Yu, Z. Dong, H.-C. Chien, Y. Shao, and N. Chi, "7-Tb/s (7×1.284 Tb/s/ch) signal transmission over 320 km using PDM-64QAM modulation," *IEEE Photon. Technol. Lett.* **24**(4), 264–266 (2012).
18. A. Sano, T. Kobayashi, S. Yamanaka, A. Matsuura, H. Kawakami, Y. Miyamoto, K. Ishihara, and H. Masuda, "102.3-Tb/s (224 × 548-Gb/s) C- and extended L-band All-Raman transmission over 240 km using PDM-64QAM single carrier FDM with digital pilot tone," in *Proceedings of OFC 2012*, paper PDP5C.3.
19. O. Bertran-Pardo, J. Renaudier, H. Mardoyan, P. Tran, R. Rios-Muller, A. Konczykowska, J.-Y. Dupuy, F. Jorge, M. Riet, B. Duval, J. Godin, S. Randel, G. Charlet, and S. Bigo, "Transmission of 50-GHz-spaced single-carrier channels at 516Gb/s over 600km," in *Proceedings of OFC 2013*, paper OTh4E.2.
20. A. Nespola, S. Straullu, G. Bosco, A. Carena, J. Yanchao, P. Poggiolini, F. Forghieri, Y. Yamamoto, M. Hirano, T. Sasaki, J. Bauwelinck, and K. Verheyen, "1306-km 20×124.8-Gb/s PM-64QAM transmission over PSCF with Net SEDP 11,300 (b-km)/s/Hz using 1.15 samp/symb DAC," in *Proceedings of ECOC 2013*, paper Th.2.D.1.
21. G. Bosco, V. Curri, A. Carena, P. Poggiolini, and F. Forghieri, "On the performance of nyquist-WDM terabit superchannels based on PM-BPSK, PM-QPSK, PM-8QAM or PM-16QAM Subcarriers," *J. Lightwave Technol.* **29**(1), 53–61 (2011).
22. R. Cigliutti, A. Nespola, D. Zeolla, G. Bosco, A. Carena, V. Curri, F. Forghieri, Y. Yamamoto, T. Sasaki, and P. Poggiolini, "16 × 125 Gb/s quasi-nyquist DAC-generated PM-16QAM transmission over 3590 km of PSCF," *IEEE Photon. Technol. Lett.* **24**(23), 2143–2146 (2012).
23. R. Schmogrow, M. Meyer, P. C. Schindler, A. Josten, S. Ben-Ezra, C. Koos, W. Freude, and J. Leuthold, "252 Gbit/s Real-Time Nyquist Pulse Generation by Reducing the Oversampling Factor to 1.33," in *Proceedings of OFC 2013*, paper OTu21.1.
24. A. Sano, T. Kobayashi, A. Matsuura, S. Yamamoto, S. Yamanaka, E. Yoshida, Y. Miyamoto, M. Matsui, M. Mizoguchi, and T. Mizuno, "100 × 120-Gb/s PDM 64-QAM transmission over 160 km using linewidth-tolerant pilotless digital coherent detection," in *Proceedings of OFC 2010*, paper PD2.4.
25. Y. Gao, A. P. T. Lau, C. Lu, J. Wu, Y. Li, K. Xu, W. Li, and J. Lin, "Low-complexity two-stage carrier phase estimation for 16-QAM systems using QPSK partitioning and maximum likelihood detection," in *Proceedings of OFC 2011*, paper OMJ6.
26. X. Zhou, L. E. Nelson, P. Magill, R. Isaac, B. Zhu, D. W. Peckham, P. I. Borel, and K. Carlson, "High spectral efficiency 400 Gb/s transmission using PDM time-domain hybrid 32–64 QAM and training-assisted carrier recovery," *J. Lightwave Technol.* **31**(7), 999–1005 (2013).
27. A. Carena, V. Curri, G. Bosco, P. Poggiolini, and F. Forghieri, "Modeling of the impact of nonlinear propagation effects in uncompensated optical coherent transmission links," *J. Lightwave Technol.* **30**(10), 1524–1539 (2012).
28. G. Bosco, R. Cigliutti, A. Nespola, A. Carena, V. Curri, F. Forghieri, Y. Yamamoto, T. Sasaki, J. Yanchao, and P. Poggiolini, "Experimental investigation of nonlinear interference accumulation in uncompensated links," *IEEE Photon. Technol. Lett.* **24**(14), 1230–1232 (2012).
29. E. Torrenco, R. Cigliutti, G. Bosco, A. Carena, V. Curri, P. Poggiolini, A. Nespola, D. Zeolla, and F. Forghieri, "Experimental validation of an analytical model for nonlinear propagation in uncompensated optical links," in *Proceedings of ECOC 2011*, paper We.7.B.2.
30. A. J. Stark, Y.-T. Hsueh, T. F. Detwiler, M. M. Filer, S. Tibuleac, and S. E. Ralph, "System performance prediction with the Gaussian noise model in 100G PDM-QPSK coherent optical networks," *J. Lightwave Technol.* **31**(21), 3352–3360 (2013).
31. P. Poggiolini, "The GN model of non-linear propagation in uncompensated coherent optical systems," *J. Lightwave Technol.* **30**(24), 3857–3879 (2012).

1. Introduction

Digital transmission systems at 100 Gb/s operated in WDM configuration based on Polarization-Multiplexed (PM) QPSK with 50 GHz channel spacing are now commercially available from several vendors. With a spectral efficiency (SE) of 2 b/s/Hz, they can reach ultra-long haul distances, up to several thousand km. During last years the focus of research has hence shifted towards substantially improving the SE, while still ensuring sufficient reach. To this end, many of the recently published papers exploit high-order QAM modulation formats and resort the Nyquist WDM (N-WDM) technique as an aggressive spectrum shaping solution to simultaneously reduce the bandwidth occupation and allow tighter channel spacing.

Recent improvements in the net spectral efficiency are shown in Fig. 1, where the main record breaking experiments of the last five years, specifically based on coherent detection and single-carrier (non-OFDM) QAM modulation, have been considered [1–20]. Trends in this figure show that any step towards high constellation order, from PM-QPSK up to PM-64QAM, generates a significant increase in net SE. Such progresses do not come for free, considering that the signal-to-noise ratios required for this higher cardinality formats, combined with the impairments due to fiber nonlinearity, limit the transmission distance [21]. Figure 2 reports the distance vs. SE for the same record experiments of Fig. 1: contour lines represent constant SE-times-distance product (SEDP) levels. While PM-QPSK outperforms all other formats in terms of SEDP and it is the clear choice for transoceanic distance over 10,000 km, PM-64QAM together with PM-16QAM can still play an important role in future flexible optical networks. In this scenario, where the system throughput may be adapted depending on the reach, PM-64QAM will be able to cover 1,000 km carrying up to 40 Tb/s over the C-band.

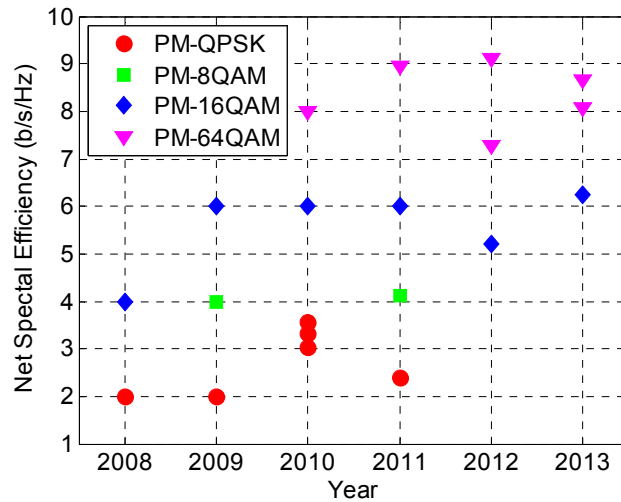


Fig. 1. Net spectral efficiency evolution of main record transmission experiments based on coherent detection published in the last five years.

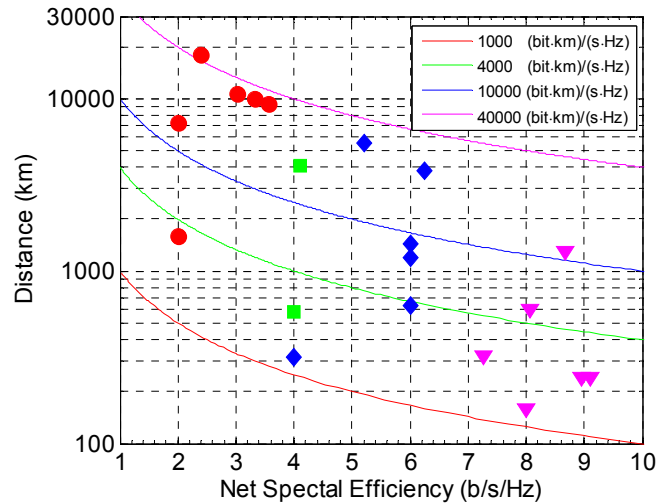


Fig. 2. System reach vs. throughput trade-off in main record transmission experiments based on coherent detection published in the last five years.

High-order format generation and N-WDM spectral shaping can both be obtained with optical techniques [4, 8], but current consensus strongly favors the use of transmitter (Tx) DSP with DACs. This powerful technology allows to generate arbitrary electrical signals to properly drive the optical modulators and simultaneously obtain an accurate high-order QAM constellation together with the desired N-WDM spectral shaping. The key component needed in this approach is a digital-to-analog converter (DAC) device, which is characterized by two main parameters: the sampling speed S_{DAC} and the number of resolution bits N_{DAC} . Typically, if S_{DAC} increases, N_{DAC} decreases. The higher is the order of the modulation format, the higher is the required value of N_{DAC} , while S_{DAC} limits the achievable symbol rate $R_s = S_{DAC}/SpS$, where SpS is the number of samples per symbol (or “oversampling factor”).

The achievable R_s can be clearly increased by decreasing the oversampling factor: research efforts have been made to decrease the value of SpS without incurring in aliasing-like penalties. In [22], a 1.5 SpS DAC-supported N-WDM PM-16QAM experiment was reported, delivering a raw SE of 7.81 b/s/Hz (net 6.48 b/s/Hz) over 3,590 km of PSCF in a submarine-system configuration. In this work we aimed at further drastically reducing the required DAC rate. At the same time, we increased the SE and constellation order to PM-64QAM, proving that this set-up could still achieve thousand-km reach in a submarine-system configuration, with a very high SE. The DAC rate was decreased to 1.15 SpS , a record-low for DSP-DAC generated N-WDM. The lowest previously reported rate was 1.33 SpS , obtained in a 100-km PM-64QAM single-channel transmission at 252 Gb/s [23]. Note that an even lower rate of 1 sample/symbol was reported in [24] but at such rate the DAC can intrinsically only generate conventional NRZ pulses, so that cascaded narrow optical filtering was needed in [24] to obtain N-WDM at the Tx output.

In addition we achieved 20-channel N-WDM transmission at 124.8 Gb/s per channel (100 Gb/s net), over 1306 km (24x54.4 km) at a raw SE of 10.4 b/s/Hz. This is the second-highest raw SE for PM-64QAM next to [18], which achieved 10.96 b/s/Hz by using a more complex transmitter structure that resorted to combining 8 lower-bit-rate PM-64QAM N-WDM subcarriers (at 68.5 Gb/s) into a single super-channel, with digital-pilot-tone assisted demodulation.

Considering a FEC overhead of 20% and thus a net SE of 8.67 b/s/Hz, the resulting net SE-times-distance product (SEDP) was 11,327 (b·km)/(s·Hz). To the best of our knowledge, this is the highest SEDP reported so far for a PM-64QAM transmission experiment.

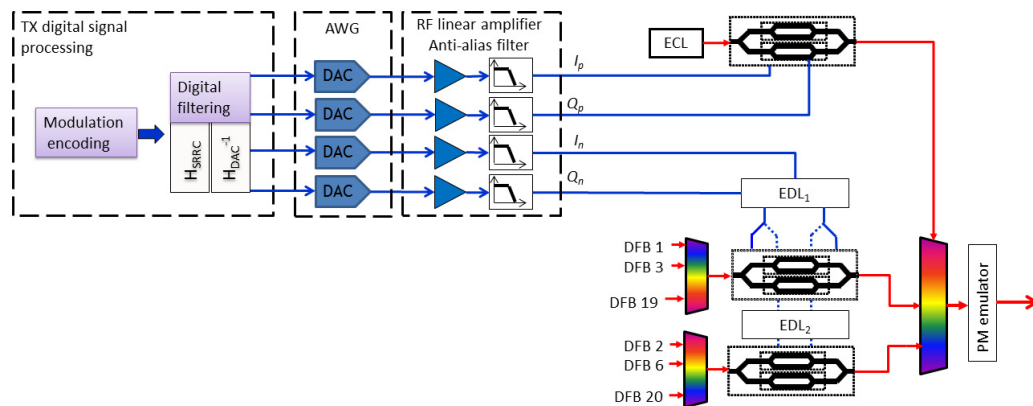


Fig. 3. Transmitter set-up for 20 PM-64QAM Nyquist-WDM channels at 10.4 Gbaud spaced 12 GHz.

2. Experimental setup

A schematic view of the transmitter setup is shown in Fig. 3. An array of 20 DFB lasers, spaced 12 GHz, was divided into odd and even carriers and separately fed to two distinct nested Mach-Zehnder modulators (NMZM). A third NMZM, fed by an external cavity laser (ECL), was used to generate the channel under test: the corresponding DFB in the array of lasers is turned off. Each of NMZMs was driven by a pair of uncorrelated signals taken from the DAC output. The DAC was a Tektronix 7122B with an analog bandwidth of 9.6 GHz, and with ten nominal resolution bits but lower Effective Number of Bits (ENOB). As shown in Fig. 3, two independent DAC output signals, called I_p and Q_p , were used to drive the NMZM for the channel under test. The four driving signals for the other two NMZMs were obtained by splitting each of the two logical complementary outputs of the DAC (I_n and Q_n). Electrical delay lines were inserted in these paths for decorrelation of interfering channel patterns: the delays EDL_1 and EDL_2 were respectively 4.8 and 4.4 ns. Each one of the in-phase and quadrature signals was created by mapping three independent ($2^{15}-1$) PRBSs into a single 8-level PAM NRZ signal at 10.4 Gbaud, which was then digitally filtered to generate a square-root raised-cosine spectrum with electrical bandwidth equal to half the symbol rate and roll-off 0.05. Note that a 4 dB high-frequency digital pre-emphasis was also applied, to partially compensate for in-band electronics attenuation.

The filtered 8-level signals were then fed to DACs which operated at 11.96 GS/s, corresponding to 1.15 SpS. As a result, an alias signal replica was also generated, centered at 11.96 GHz (Fig. 4(a)). It was partially filtered out by the low-pass frequency response of the DAC, but, in order to further suppress it, a specifically-designed anti-alias (AA) filter, with steep cut-off, was interposed between the DAC and the modulators. The AA filter frequency response is shown in Fig. 4(a) with a red dashed line. The spectrum of the NMZM driving signal, cleaned out of the signal replica, is reported in Fig. 4(b). Not shown for clarity, the AA filter response goes back up to -20 dB at about 15 GHz, but this causes no adverse effect because the signal components at such frequencies are very low.

Preceding the AA filters, broadband RF amplifiers were used to obtain a peak to peak amplitude voltage of about 25% of the modulator V_{π} , so as to operate them in linearity. All the modulated optical channels, so far single-polarization, were then coupled together and sent into a commercial PM emulator with a 10 ns polarization decorrelation delay.

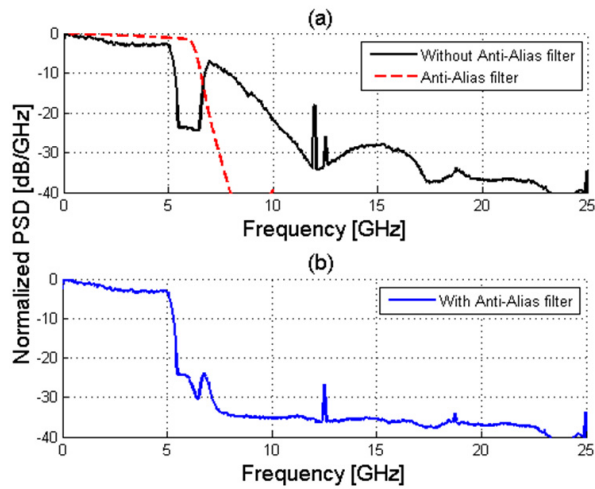


Fig. 4. Spectrum of the modulator-driving signal (8-level NRZ PAM) with (a) and without (b) anti-alias filter. In (a) the red dashed line is the anti-alias filter transfer function.

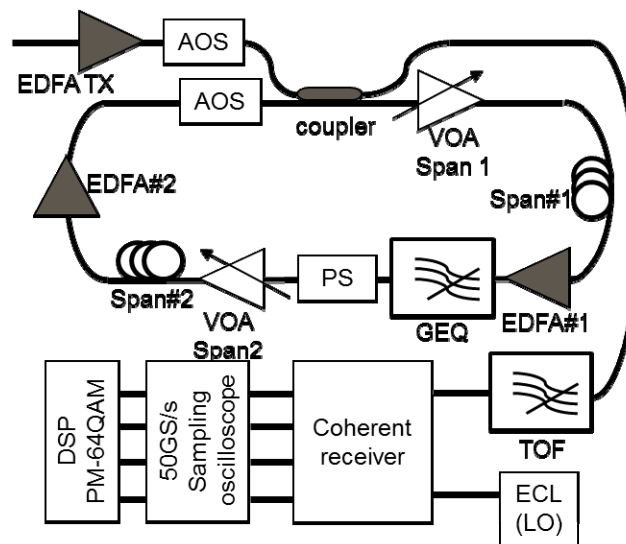


Fig. 5. Recirculating loop structure and receiver layout.

The transmission link, depicted in Fig. 5, consists of a re-circulating loop with two identical 54.44 km spans of uncompensated PSCF. At 1550 nm, the average fiber loss was 0.161 dB/km, chromatic dispersion 20.7 ps/nm/km and effective area $150 \mu\text{m}^2$. The total loss of each span was 9.7 dB, resulting from a combination of fiber loss and splicing loss between standard single-mode fiber and the large-effective-area PSCF. The loop made use of EDFA-only amplification. It included a spectrally-resolved gain equalizer (GEQ) and a loop-synchronous polarization scrambler (PS) to, respectively, compensate for the EDFA gain-tilt and ripples and effectively average the impact of polarization effects. The EDFA noise figure was 4.5 dB.

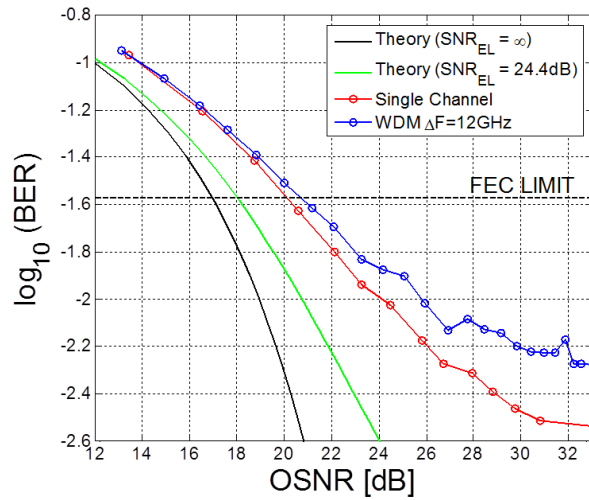


Fig. 6. Back-to-back performance: BER vs. OSNR (over 0.1 nm).

At the receiver (Fig. 5), the WDM comb was sent into a tunable optical filter (TOF) with 30 GHz bandwidth to limit to total amount of power entering in the photo-detectors. The filtered signal was subsequently fed to a standard coherent receiver, where the signal was mixed with the local oscillator, obtained from a tunable ECL of linewidth 100-kHz, different from the one used at the Tx. The four electrical outputs of the receiver front-end were digitized using a 50 GS/s real-time oscilloscope (Tektronix DPO71604). Finally, offline DSP was used to demodulate the resulting samples.

The DSP consisted of the following stages: a down-converting stage that lowers the sample-rate to 2 SpS; a chromatic dispersion compensation stage implemented using a pair of complex FIR filters; a frequency offset compensator; a first 2x2 complex MIMO equalizer with 21 taps that adjusts its coefficient through a multi-modulus CMA algorithm (initialized with a training sequence and then switched to blind radius-directed operation); a Maximum-Likelihood carrier phase-recovery (CPE) stage [25] and a final decision-directed LMS 4x4 equalizer with 51 taps.

3. Results

The back-to-back performance in terms of BER vs. OSNR (defined over a 0.1-nm bandwidth), is shown in Fig. 6. We assumed to employ a soft-decision LDPC convolutional code with 20% overhead and layered decoding algorithm [26], corresponding to a FEC BER threshold equal to $2.7 \cdot 10^{-2}$ ($Q^2 = 5.7$ dB). The penalty between single-channel and WDM at FEC threshold is only 0.4 dB, confirming that DAC-enabled spectral shaping and the use of steep electrical anti-alias filters effectively curtails inter-channel linear crosstalk, allowing an extremely tight channel spacing. The penalty in WDM conditions with respect to theory at FEC threshold amounts to 3.6 dB. It is due to a combination of electrical and optical component non-idealities, with main contributors the limited effective number of bit of DAC and oscilloscope, the transmitter RF broadband amplifiers noise and the electrical circuitry reflections due to impedance mismatch. In order to quantify the amount of penalty due to electrical components only, we tested the system in an electrical back-to-back configuration, connecting the AA filter output directly to the real-time oscilloscope. The measured BER was found to be equal to 10^{-4} while the corresponding electrical SNR, verified by measuring EVM on the scattering diagram, was equal to 24.4 dB. Taking analytically into account such contribution, we derived the actual theoretical baseline for our system (shown in Fig. 6 as a

green solid line) and we concluded that, at FEC threshold, the contribution of the electrical non idealities to the total penalty is 1 dB. The additional penalties, not measurable with the back-to-back electrical configuration, are due to some remaining non-idealities such as the electro-optical bandwidth of modulators, the electrical bandwidth and noise of the coherent receiver and the most important impedance mismatch between the anti-alias filter and the electrical ports of modulators.

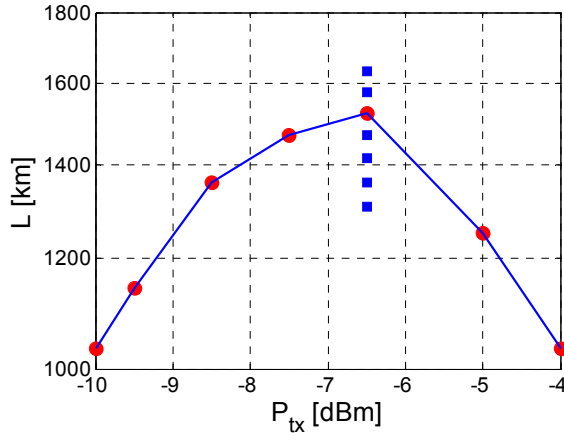


Fig. 7. Maximum reach of the center channel (#11) at FEC threshold as a function of the power level (red dots). Maximum reach for all the 20 channels at optimal power level of -6.5 dBm (blue squares). Distances are quantized over a discrete number of spans of length equal to 54.44 km.

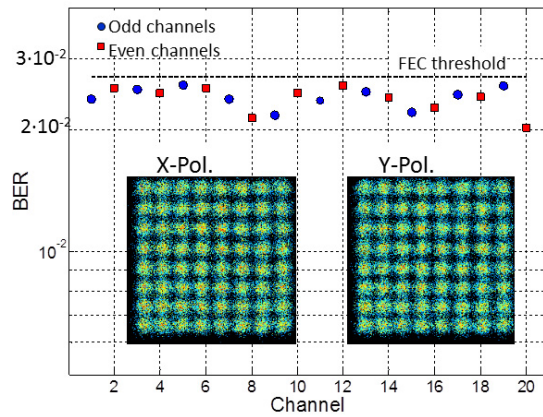


Fig. 8. BER for all 20 channels at 24 spans (1306 Km). Inset: signal constellations (both polarizations) for channel #11.

WDM transmission experiments were then performed, carrying out a first set of measurements in order to optimize the launch power. In Fig. 7 we report the maximum reachable distance for the center channel (#11) at FEC threshold as a function of the transmitted power levels (red dots). At the optimum launch power, that was found to be -6.5 dBm per channel, channel #11 showed a maximum reach of 28 spans for a total of 1523 km. Having defined the optimum power per channel, we carried out the measurement of the maximum reach for all channels, shown in Fig. 7 as blue squares. All channels have quite similar performance with a maximum reached distance that ranges from a minimum value of

1306 km (24 spans) to a max of 1632 km (30 spans). The observed differences are due to a residual unbalancing in channel power in the order of ± 0.5 dB that results in different OSNR in each channel.

Figure 8 shows the BER values measured for all 20 WDM channels at optimum power after 24 spans (1306 km): at this distance the BERs of all channels fall below the FEC threshold. In the same figure we also reported, in the inset, the signal constellations after transmission over 1306 km for the center channel (#11) and for both polarizations.

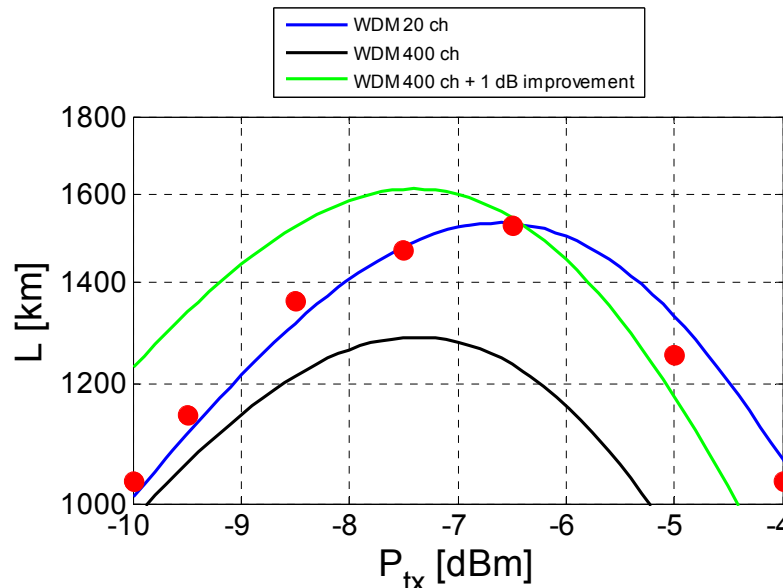


Fig. 9. Maximum reach prediction based on the GN-model under different conditions: 20 and 400 WDM channels. Red dots: experimental measurement on the center channel of the WDM comb.

4. GN-model prediction

The experiment carried out was limited to 20 WDM channels, due to lack of DFB sources in the lab inventory: in this section we want to predict the potential performance of PM-64QAM when loading the entire C-band using the GN-model for nonlinear propagation in uncompensated coherent optical systems [27], that has been recently experimentally validated by independent groups [14, 28–30]. We first identified the parameters for this specific experimental setup and verified that the model is able to predict the performance for the 20 channels scenario. In Fig. 9 we report the GN-model prediction for the 20 WDM case together with measurements taken for the center channel, whose performance is close to the average of all the WDM comb (see Figs. 7 and 8). As expected, we found a very good agreement between GN-model and measurements.

We then used the GN-model to predict the system performance under different conditions. First, we estimated the maximum reach when the full C-band is loaded, keeping all other parameters fixed. At a channel spacing of 12 GHz, it corresponds to 400 channels, for a total net system throughput of 40 Tb/s (400 x 100 Gb/s). As shown in [31], the NLI interference increment with respect to the number of channels follows approximately a logarithmic law, thus the loss in performance when moving to the full C-band should not be dramatic, but not negligible, as well: the black solid line in Fig. 9 shows that the maximum distance is decreased from 1523 to 1306 km, at an optimum launch power of -7.4 dBm.

This result was obtained assuming the same Tx/Rx performance of the experimental set-up, that, at the reference BER of $2.7 \cdot 10^{-2}$, was affected by 3.6 dB of penalty with respect to theory (see Fig. 6). An optimized transceiver design together with device integration will surely be able to deliver an improved back-to-back performance. Assuming a 1-dB OSNR improvement with respect to our Tx/Rx pair, the maximum reach would increase to 1632 Km (30 spans), as shown as the green solid line in Fig. 9. Such results clearly show that PM-64QAM, even considering adequate system margin in actual field deployment, can reach over 1,000 km offering a 40 Tb/s throughput in EDFA-only configurations based solely on C-band.

5. Conclusions

We have demonstrated the transmission of 20x124.8 Gb/s Nyquist-WDM channels, based on PM-64QAM modulation with 12 GHz channel spacing, over 1306 km of PSCF, in an EDFA-only submarine-like set-up. All channels were below FEC threshold after propagating over 24 spans of PSCF fiber, each 54.4 km long. The net spectral efficiency was 8.67 b/s/Hz and the spectral efficiency distance product was a record 11,327 (b·km)/(s·Hz) for PM-64QAM channels with throughput higher than 100 Gb/s.

Digital spectral shaping at the transmitter and the use of suitable anti-alias filters had a strong impact on the system performance: despite the DAC sampling speed was a record-low 1.15 SpS, the system was able to operate at very narrow channel spacing with negligible linear crosstalk between channels.

Our back-to-back results indicate that there is still margin for sensitivity improvement, which could be likely achieved by integrated transmitter electronics design. GN-model predictions clearly indicate, with a proven degree of reliability, that Nyquist-WDM PM-64QAM is a realistic option for ultra-high capacity transmission up to a total throughput of 40 Tb/s in the C-band for 1,000 km range, in a submarine configuration based on EDFA only.

Acknowledgments

This work was supported by CISCO Systems within a SRA contract. We thank OCLARO for supplying the NMZ modulators.